Newsjournal of the Society for Industrial and Applied Mathematics
sinews.siam.org

siam news

Volume 53/ Issue 9
November 2020

Special Issue on the Mathematics of Planet Earth

*Read about the application of mathematics and computational science to issues concerning invasive populations, Arctic sea ice, insect flight, and more in this Planet Earth **special issue**!*

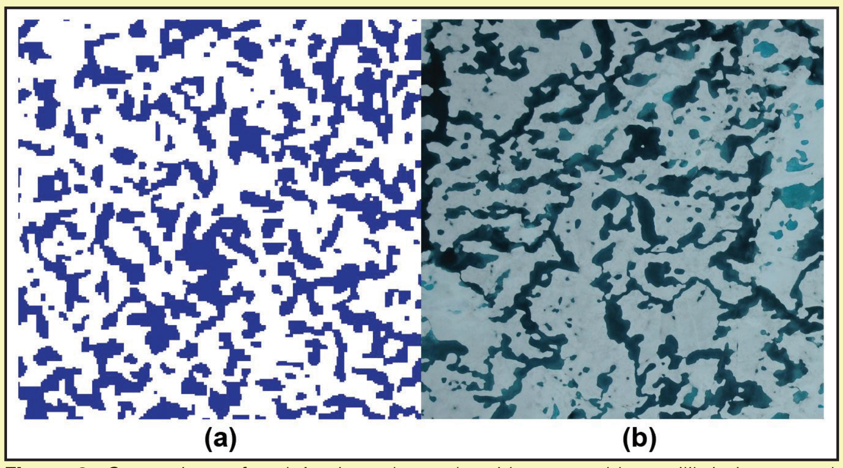

Figure 3. *Comparison of real Arctic melt ponds with metastable equilibria in our melt pond Ising model.* **3a.** *Ising model simulation.* **3b.** *Real melt pond photo. Figure 3a courtesy of Yiping Ma, 3b courtesy of Donald Perovich.*

Vast labyrinthine ponds on the surface of melting Arctic sea ice are key players in the polar climate system and upper ocean ecology. Researchers have adapted the Ising model, which was originally developed to understand magnetic materials, to study the geometry of meltwater's distribution over the sea ice surface. In an article on page 5, Kenneth Golden, Yiping Ma, Courtenay Strong, and Ivan Sudakov explore model predictions.

Controlling Invasive Populations in Rivers

By Yu Jin and Suzanne Lenhart

Flow regimes can change significantly over time and space and strongly impact all levels of river biodiversity, from the individual to the ecosystem. Invasive species in rivers—such as bighead and silver carp, as well as quagga and zebra mussels—continue to cause damage. Management of these species may include targeted adjustment of flow rates in rivers, based on recent research that examines the effects of river morphology and water flow on rivers' ecological statuses. While many previous methodologies rely on habitat suitability models or oversimplification of the hydrodynamics, few studies have focused on the integration of ecological dynamics into water flow assessments.

Earlier work yielded a hybrid modeling approach that directly links river hydrology with stream population models [3]. The hybrid model's hydrodynamic component is based on the water depth in a gradually varying river structure. The model derives the steady advective flow from this structure and relates it to flow features like water discharge, depth, velocity, cross-sectional area, bottom roughness, bottom slope, and gravitational acceleration. This approach facilitates both theoretical understanding and the generation of quantitative predictions, thus providing a way for scientists to analyze the effects of river fluctuations on population processes.

When a population spreads longitudinally in a one-dimensional (1D) river with spatial heterogeneities in habitat and temporal fluctuations in discharge, the resulting hydrodynamic population model is

$$N_t = -A_t(x,t)\frac{N}{A(x,t)} + \frac{1}{A(x,t)}\Big(D(x,t)A(x,t)N_x\Big)_x - \frac{Q(t)}{A(x,t)}N_x + rN\left(1-\frac{N}{K}\right)$$

$$\begin{aligned} &N(0,t)=0 && \text{on } (0,T), x=0,\\ &N_x(L,t)=0 && \text{on } (0,T), x=L,\\ &N(x,0)=N_0(x) && \text{on } (0,L), t=0 \end{aligned} \quad (1)$$

See **Invasive Populations** *on page 4*

Modeling Resource Demands and Constraints for COVID-19 Intervention Strategies

By Erin C.S. Acquesta, Walt Beyeler, Pat Finley, Katherine Klise, Monear Makvandi, and Emma Stanislawski

As the world desperately attempts to control the spread of COVID-19, the need for a model that accounts for realistic trade-offs between time, resources, and corresponding epidemiological implications is apparent. Some early mathematical models of the outbreak compared trade-offs for non-pharmaceutical interventions [3], while others derived the necessary level of test coverage for case-based interventions [4] and demonstrated the value of prioritized testing for close contacts [7].

Isolated analyses provide valuable insights, but real-world intervention strategies are interconnected. Contact tracing is the lynchpin of infection control [6] and forms the basis of prioritized testing. Therefore, quantifying the effectiveness of contact tracing is crucial to understanding the real-life implications of disease control strategies.

Contact Tracing Demands

Contact tracers are skilled, culturally competent interviewers who apply their knowledge of disease and risk factors when notifying people who have come into contact with COVID-19-infected individuals. They also continue to monitor the situation after case investigations [1].

Case investigation consists of four steps:

1. Identify and notify cases
2. Interview cases
3. Locate and notify contacts
4. Monitor contacts.

Most health departments are implementing case investigation, contact identification, and quarantine to disrupt COVID-19 transmission. The timeliness of contact tracing is constrained by the length of the infectious period, the turn-around time for testing and result reporting, and the ability to successfully reach and interview patients and their contacts. The European Centre for Disease Prevention and Control approximates that contact tracers spend one to two hours conducting an interview [2]. Estimates regarding the timelines of other steps are limited to subject matter expert elicitation and can vary based on cases' access to phone service or willingness to participate in interviews.

Bounded Exponential

The fundamental structure of our model follows traditional susceptible-exposed-infected-recovered (SEIR) compartmental modeling [5]. We add an asymptomatic population A, a hospitalized population H, and disease-related deaths D, as well as corresponding quarantine states. We define the states $\{S_i, E_i, A_i, I_i, H, R, D\}_{i=0,1}$ for our compartments, such that $i=0$ and $i=1$ correspond to unquarantined and quarantined respectively. Rather than focus on the dynamics that are associated with the state transition diagram in Figure 1, we introduce a formulation for the real-time demands on contact tracers' time as a function of infection prevalence, while also respecting constraints on resources.

When the work that is required to investigate new cases and monitor existing contacts exceeds available resources, a backlog develops. To simulate this backlog, we introduce a new compartment C for tracking the dynamic states of cases:

$$\frac{dC}{dt} = [flow_{in}] - [flow_{out}].$$

Flow into the backlog compartment, represented by $[flow_{in}]$, reflects case identification that is associated with the following transitions in the model:

– The rate of random testing: $q_{rA}(t)A_0(t) \to A_1(t)$ and $q_{rI}(t)I_0(t) \to I_1(t)$

– Testing triggered by contact tracing: $q_{tA}(t)A_0(t) \to A_1(t)$, $q_{tI}(t)I_0(t) \to I_1(t)$, and $q_{tE}(t)E_1(t) \to \{A_1(t), I_1(t)\}$

– The population that was missed by the non-pharmaceutical interventions that require hospitalization: $\tau_{IH}(t)I_0(t) \to H(t)$.

Here, $q_{r*}(t)$ defines the time-dependent rate of random testing, $q_{t*}(t)$ signifies the time-dependent rate of testing that is triggered by contact tracing, and τ_{IH} is the inverse of the expected amount of time for which an infected individual is symptomatic before hospitalization. These terms collectively provide the simulated number of newly-identified positive COVID-19 cases. However, we also need the average number of contacts per case. We thus define function $\mathcal{K}(\kappa, T_S, \phi_\kappa)$ that depends on the average number of contacts a day (κ), the average number of days for which an individual is infectious before going into isolation (T_S), and the likelihood that the individual

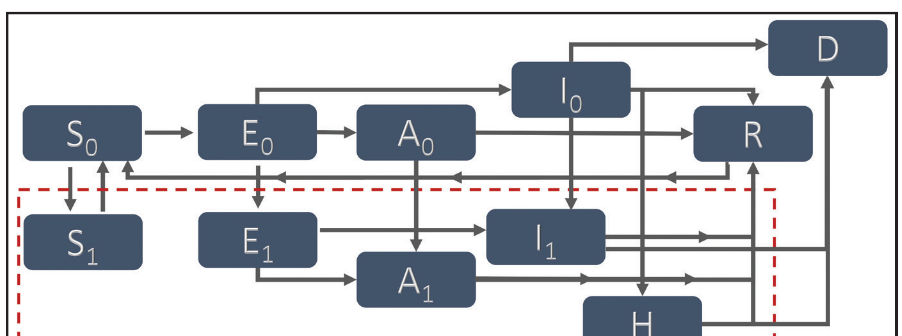

Figure 1. *Disease state diagram for the compartmental infectious disease model. Figure courtesy of the authors.*

See **COVID-19 Intervention** *on page 3*

Nonprofit Org
U.S. Postage
PAID
Permit No 360
Bellmawr, NJ

siam
SOCIETY for INDUSTRIAL and APPLIED MATHEMATICS
3600 Market Street, 6th Floor
Philadelphia, PA 19104-2688 USA

From Magnets to Melt Ponds

By Kenneth M. Golden, Yiping Ma, Courtenay Strong, and Ivan Sudakov

When the snow on top of Arctic sea ice begins to melt in late spring, small pools of water form on the surface. As the melt season progresses, these simply shaped meter-scale pools grow and coalesce into kilometer-scale labyrinths of cerulean blue with complex, self-similar boundaries. The fractal dimension of these boundaries transitions from one to roughly two as the area increases through a critical regime that is centered around 100 square meters [4]. While the white, snowy surface of the sea ice reflects most of the incident sunlight, the darker melt ponds act like windows and allow significant light to penetrate the ice and seawater underneath. Melt ponds thus help control the amount of solar energy that the ice pack and upper ocean absorb, strongly influencing ice melting rates and the ecology of the polar marine environment. They largely determine sea ice albedo—the ratio of reflected to incident sunlight—which is a key parameter in climate modeling.

When viewed from a helicopter, the beautiful patterns of dark and light on the surface of melting sea ice are reminiscent of structures that applied mathematicians sometimes see when studying phase transitions and coarsening processes in materials science. They also resemble the complex regions of aligned spins, or *magnetic domains*, that are visible in magnetic materials. Figure 1 compares two examples of magnetic domains with similar patterns that are formed by melt ponds on Arctic sea ice. Magnetic energy is lowered when nearby spins align with each other, which produces the domains. At higher temperatures, thermal fluctuations dominate the tendency of the domains' magnetic moments to also align, with no net magnetization M of the material unless one applies an external magnetic field H to induce alignment. However, the tendency for overall alignment takes over at temperatures below the Curie point T_c, and the material remains magnetized even as the applied field H vanishes, where the remaining non-zero magnetization $(M \neq 0)$ is called *spontaneous* or *residual*.

The prototypical model of a magnetic material based on a lattice of interacting binary spins is the Ising model, which was proposed in 1920 by Ernst Ising's Ph.D. advisor Wilhelm Lenz. This model incorporates only the most basic physics of magnetic materials and operates on the principle that natural systems tend toward minimum energy states.

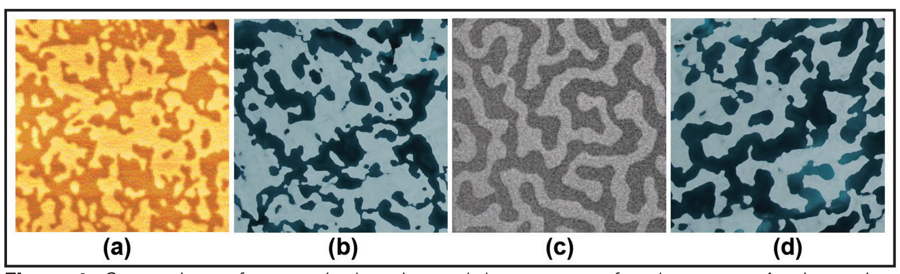

Figure 1. *Comparison of magnetic domains and the patterns of meltwater on Arctic sea ice.* **1a.** *Magnetic domains in cobalt, roughly 20 microns across.* **1b.** *Arctic melt pond, roughly 100 meters across.* **1c.** *Magneto-optic Kerr effect microscope image of maze-like domain structures in thin films of cobalt-iron-boron, roughly 150 microns across.* **1d.** *Similarly-structured melt ponds, roughly 70 meters across. Figure 1a courtesy of [9], 1b and 1d courtesy of Donald Perovich, 1c courtesy of [10].*

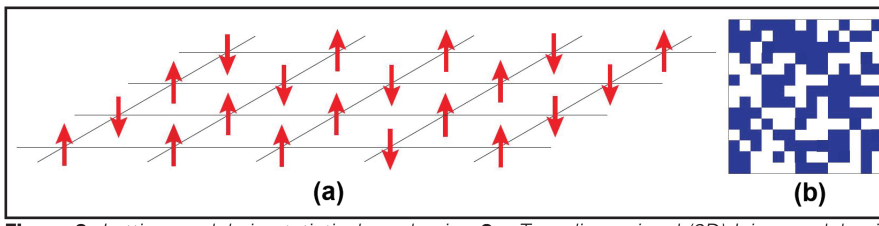

Figure 2. *Lattice models in statistical mechanics.* **2a.** *Two-dimensional (2D) Ising model, with spins either up or down at each lattice site.* **2b.** *Spin configuration. Spin-up sites are blue and spin-down sites are white. Image courtesy of Kenneth Golden.*

Consider a finite box $\Lambda \subset \mathbb{Z}^2$ that contains N sites. At each site, a spin variable s_i can take the values $+1$ or -1 (see Figure 2). To illustrate our melt pond Ising model, we formulate the problem of finding the magnetization $M(T,H)$—or *order parameter*—of an Ising ferromagnet at temperature T in field H. The Hamiltonian $\mathcal{H}$ with ferromagnetic interaction $J \geq 0$ between nearest neighbor pairs is given by

$$\mathcal{H}_\omega = -H\sum_i s_i - J\sum_{<i,j>} s_i s_j$$

for any configuration $\omega \in \Omega = \{-1,1\}^N$ of the spin variables. The canonical partition function Z_N, which yields the system's observables, is given by

$$Z_N(T,H) = \sum_{\omega\in\Omega} \exp(-\beta\mathcal{H}_\omega) = \exp(-\beta N f_N),$$

where $\beta = 1/kT$, k is Boltzmann's constant, $\exp(-\beta\mathcal{H}_\omega)$ is the Gibbs factor, and f_N is the free energy per site: $f_N(T,H) = (-1/\beta N)\log Z_N(T,H)$.

The magnetization $M(T,H) = \lim_{N\to\infty} \frac{1}{N}\sum_i s_i$ is averaged over $\omega\in\Omega$ with Gibbs' weights and expressed in terms of the free energy $f(T,H) = \lim_{N\to\infty} f_N(T,H)$:

$$M(T,H) = -\frac{\partial f}{\partial H}.$$

The model's rich behavior is exemplified in the existence of a critical temperature T_c—the Curie point—where $M(T) = \lim_{H\to 0} M(T,H) > 0$ for $T < T_c$ and $M(T) = 0$ for $T \geq T_c$. Universal power law asymptotics for $M(T) \to 0$ as $T \to T_c^-$ are independent of the lattice type and other local details.

The Metropolis algorithm is a common method for numerically constructing equilibrium states of the Ising ferromagnet. In this approach, a randomly-chosen spin either flips or does not flip based on which action lowers or raises the energy. ΔE represents the change in magnetostatic energy from a potential flip (as measured by $\mathcal{H}_\omega$), and the spin is flipped if $\Delta E \leq 0$. If $\Delta E > 0$, the probability of the spin flipping is given by the Gibbs factor for ΔE. Sweeping through the whole lattice and iterating the process many times attains a local minimum in the system's energy.

We have adapted the classical Ising model to study and explain the observed geometry of melt pond configurations and capture the fundamental physical mechanism of pattern formation in melt ponds on Arctic sea ice [5]. While previous studies have developed important and instructive numerical models of melt pond evolution [2, 3],

See **Melt Ponds** *on page 7*

Melt Ponds

Continued from page 5

these models were somewhat detailed and did not focus on the way in which meltwater is distributed over the sea ice surface. Our new model is simplistic and accounts for only the system's most basic physics. In fact, the only measured parameter is the one-meter lattice spacing, which is determined by snow topography data.

The simulated ponds are metastable equilibria of our melt pond Ising model. They have geometrical characteristics that agree very closely with observed scaling of pond sizes [6] and the transition in pond fractal dimension [4]. Researchers have also developed continuum percolation models that reproduce these geometrical features [1, 8].

We aim to use our Ising model to introduce a predictive capability to cryosphere modeling based on ideas of statistical mechanics and energy minimization, utilizing just the essential physics of the system. The model consists of a two-dimensional lattice of N square patches, or pixels, of meltwater $(s_i = +1)$ or ice $(s_i = -1)$, which correspond to the spin-up or spin-down states in the Ising ferromagnet. Configurations $\omega \in \Omega = \{-1, 1\}^N$ of the spin field s_i represent the distribution of meltwater on the sea ice surface. Each patch interacts only with its nearest neighbors and is influenced by a forcing field. However, sea ice surface topography—which can vary from site to site and influence whether a patch comprises water or ice—plays the role of the applied field in our melt pond Ising model. Our model is then actually a *random field* Ising model, and one can write the Hamiltonian as

$$\mathcal{H}_\omega = -\sum_i (H - h_i) s_i - J \sum_{<i,j>} s_i s_j.$$

Here, h_i are the surface heights (taken to be independent Gaussian variables with mean zero) and H is a reference height (taken to be zero in the model's simplest form). The spin field s_i is reorganized to lower the free energy, and the order parameter is the pond area fraction $F = (M+1)/2$, which is directly related to sea ice albedo. We set temperature $T = 0$ and assume for simplicity that environmental noise does not significantly influence melt pond geometry.

Independent flips of a weighted coin determine the system's initial random configuration. A pixel or site has a probability p of its spin being $+1$, or meltwater. The system then updates based on simple rules: pick a random site i and update s_i as follows. If a majority exists among s_i's four nearest neighbors, we assume that heat diffusion drives s_i to agree with this majority. Otherwise we assume water's tendency to fill troughs, as determined by the local value of the random field h_i. This update step, which corresponds to energy minimization via Glauber spin flip dynamics, iterates until s_i becomes steady. The spin-up or meltwater clusters in the final configurations of the spin field s_i exhibit geometric characteristics that agree surprisingly well with observations of Arctic melt ponds (see Figure 3, on page 1). The final configuration is a metastable state — a local minimum of $\mathcal{H}_\omega$. As neighboring sites exchange heat, spins tend to align to minimize energy. In doing so, they coarsen away from the purely random initial state. The emergence of this order from disorder is a central theme in statistical physics and an attractive feature of our approach.

The ability to efficiently generate realistic pond spatial patterns may enable advances in how researchers account for melt ponds and many related physical and biological processes in global climate models (GCMs). Typical GCM grid spacing is tens to hundreds of kilometers, so melt ponds are subgrid-scale and thus too small to resolve on the model grid. Instead, GCMs use *parameterizations* to specify a pond fraction. Specifically, modern parameterizations in GCMs track a thermodynamically-driven meltwater volume and distribute it over the sea ice thickness classes that are present in a grid cell, beginning with the thinnest class since it presumably has the lowest ice height [3]. This yields a pond fraction F and a first-order approximation to sea ice albedo, $\alpha_{sea\ ice} = F\alpha_{water} + (1-F)\alpha_{snow}$, but does not address how the pond's area is organized spatially. Our simple model provides a framework for prescribing a subgrid-scale spatial organization whose realistic fractal dimension or area-perimeter relation could have important influences on pond evolution [7].

At this stage, total agreement between this simple model and the real world is too much to ask. The Ising model is unable to resolve features that are smaller than the lattice constant, and the metastable state also inherits certain unrealistic features from the purely random initial condition. Nonetheless, the model may be able to use more sophisticated rules to reproduce actual melt pond evolution. We anticipate that emerging techniques—like machine learning—will deduce such evolutionary rules from observational data.

References

[1] Bowen, B., Strong, C., & Golden, K.M. (2018). Modeling the fractal geometry of Arctic melt ponds using the level sets of random surfaces. *J. Fract. Geom.*, *5*, 121-142.

[2] Flocco, D., & Feltham, D.L. (2007). A continuum model of melt pond evolution on Arctic sea ice. *J. Geophys. Res.*, *112*, C08016.

[3] Flocco, D., Feltham, D.L., & Turner, A.K. (2010). Incorporation of a physically based melt pond scheme into the sea ice component of a climate model. *J. Geophys. Res.*, *115*(C8), C08012.

[4] Hohenegger, C., Alali, B., Steffen, K.R., Perovich, D.K., & Golden, K.M. (2012). Transition in the fractal geometry of Arctic melt ponds. *The Cryosphere*, *6*(5), 1157-1162.

[5] Ma, Y.P., Sudakov, I., Strong, C., & Golden, K.M. (2019). Ising model for melt ponds on Arctic sea ice. *New J. Phys.*, *21*, 063029.

[6] Perovich, D.K., Tucker, W.B., & Ligett K. (2002). Aerial observations of the evolution of ice surface conditions during summer. *J. Geophys. Res.*, *107*(C10), C000449.

[7] Polashenski, C., Perovich, D., & Courville, Z. (2012). The mechanisms of sea ice melt pond formation and evolution. *J. Geophys. Res.*, *117*(C1), C01001.

[8] Popović, P., Cael, B.B., Silber, M., & Abbot, D.S. (2018). Simple rules govern the patterns of Arctic sea ice melt ponds. *Phys. Rev. Lett.*, *120*(14), 148701.

[9] Portland Waldorf School. (2008). Electromagnetism. Retrieved from http://www.alchemical.org/em/index.html.

[10] Yamanouchi, M., Jander, A., Dhagat, P., Ikeda, S., Matsukura, F., & Ohno, H. (2011). Domain structure in CoFeB thin films with perpendicular magnetic anisotropy. *IEEE Magn. Lett.*, *2*, 3000304.

Kenneth M. Golden is a distinguished professor of mathematics and an adjunct professor of biomedical engineering at the University of Utah. His research is focused on developing mathematics of composite materials and statistical physics to model sea ice structures and processes. Yiping Ma is a Vice Chancellor's Fellow of Mathematics at Northumbria University. His research focuses on nonlinear dynamics and statistical physics with applications to diverse areas, including materials, optics, climate, and fluids. Courtenay Strong is an associate professor of atmospheric sciences at the University of Utah. A substantial component of his research focuses on modeling and analysis of the cryosphere, which includes sea ice and snow. Ivan Sudakov is an assistant professor in the Department of Physics at the University of Dayton and a Kavli Institute for Theoretical Physics Scholar. He specializes in data analysis and mathematical modeling for physical and living systems.